

Understanding Disease Control: Influence of Epidemiological and Economic Factors

Katarzyna Oleś^{1,2*}, Ewa Gudowska-Nowak¹, Adam Kleczkowski²

1 M. Kac Complex Systems Research Center and M. Smoluchowski Institute of Physics, Jagiellonian University, Kraków, Poland, **2** Department of Computing Science and Mathematics, University of Stirling, Stirling, United Kingdom

Abstract

We present a model of disease transmission on a regular and small world network and compare different control options. Comparison is based on a total cost of epidemic, including cost of palliative treatment of ill individuals and preventive cost aimed at vaccination or culling of susceptible individuals. Disease is characterized by pre-symptomatic phase, which makes detection and control difficult. Three general strategies emerge: global preventive treatment, local treatment within a neighborhood of certain size and only palliative treatment with no prevention. While the choice between the strategies depends on a relative cost of palliative and preventive treatment, the details of the local strategy and, in particular, the size of the optimal treatment neighborhood depend on the epidemiological factors. The required extent of prevention is proportional to the size of the infection neighborhood, but depends on time till detection and time till treatment in a non-linear (power) law. The optimal size of control neighborhood is also highly sensitive to the relative cost, particularly for inefficient detection and control application. These results have important consequences for design of prevention strategies aiming at emerging diseases for which parameters are not necessarily known in advance.

Citation: Oleś K, Gudowska-Nowak E, Kleczkowski A (2012) Understanding Disease Control: Influence of Epidemiological and Economic Factors. PLoS ONE 7(5): e36026. doi:10.1371/journal.pone.0036026

Editor: Yamir Moreno, University of Zaragoza, Spain

Received: October 3, 2011; **Accepted:** March 26, 2012; **Published:** May 9, 2012

Copyright: © 2012 Oleś et al. This is an open-access article distributed under the terms of the Creative Commons Attribution License, which permits unrestricted use, distribution, and reproduction in any medium, provided the original author and source are credited.

Funding: Project operated within the Foundation for Polish Science International Ph.D. Projects Programme co-financed by the European Regional Development Fund covering, under the agreement no. MPD/2009/6, the Jagiellonian University International Ph.D. Studies in Physics of Complex Systems. The project was carried out within the MPD programme "Physics of Complex Systems" of the Foundation for Polish Science and cofinanced by the European Development Fund in the framework of the "Innovative Economy Programme" and within the framework of "Exploring the Physics of Small Devices (EPSD)" of European Science Foundation (ESF). The funders had no role in study design, data collection and analysis, decision to publish, or preparation of the manuscript.

Competing Interests: The authors have declared that no competing interests exist.

* E-mail: kas@cs.stir.ac.uk

Introduction

The network-based approaches are a common tool in epidemiological studies [1]. These individual-based methodologies allow incorporating the diverse patterns of interaction that underlie disease transmission and have been proved to capture topology of populations [2,3]. An interesting aspect of such studies, with an obvious goal to target spread of the disease, is identification of optimal strategies for the control of a disease under additional constraints [4–6]. Network modelling has been successfully used for many systems in order to design such control strategies [7]. However, there are only very few attempts to incorporate economic factors in such realistic models. Conversely, bioeconomic models usually ignore the spatial components of the disease spread [8–10].

In this paper we present a combined epidemiological and economic model to address the problem of optimization of disease control on networks with incomplete knowledge. Two main sources of costs can be associated with a disease outbreak and its control: the palliative cost associated with disease case and costs of measures aimed at preventing further cases [11,12]. The objective of preventive actions is to lower the total cost by investing e.g. in vaccination at the initial stages of the epidemic or culling of infected/susceptible individuals.

In our approach, we define a measure of the total cost of the epidemic (the severity index, X) and analyze the influence of the

parameters on its minimum. Work so far has shown that it is possible in such models to find an optimal control strategy [12]. Three optimal control scenarios (Global Strategy (GS), Local Strategy (LS), Null Strategy (NS)) emerge from the cost-effectiveness analysis. However, the relationship between the details of the Local Strategy and the model parameters is still elusive [7,12]. Establishing such a relationship is an essential step in designing control strategies for emerging diseases and hence we have concentrated on this task in the paper. We investigate propagation of the disease in a small-world network. The basic topology represents a regular lattice, with additional long-range bonds between randomly chosen pairs of sites. Inclusion of shortcuts into a regular lattice enhances communication of the disease and causes proliferation of epidemics at locations far apart from the original infected source.

Our principal objective is to identify optimal strategies for eradication of the disease by determining the threshold size of the control neighborhood. In the proposed model, the neighborhood order z is introduced as a measure of either the distance that the disease can spread (epidemic neighborhood), or the spatial extension of the control measures in a single "event" (control neighborhood). To investigate how limited resources should be balanced between disease detection and eradication, we analyze combined effects of the average time until detection and the treatment rate on optimal control size of the neighborhood.

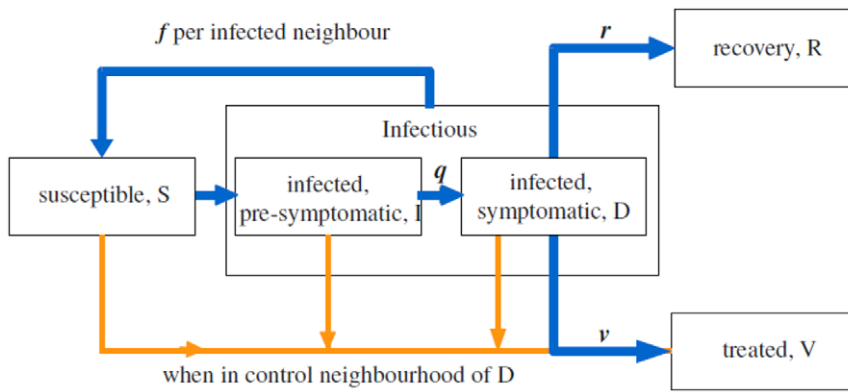


Figure 1. Block diagram illustrating transitions in the model: transitions performed at each time step (blue solid lines) and transitions triggered by treatment (orange thin lines).
doi:10.1371/journal.pone.0036026.g001

We have found that the scale of control matches the scale of dispersal of a disease and so the larger the infection neighborhood, the further the control has to be extended. This relationship can be approximated by a linear function which coefficients depend algebraically on the detection and treatment rates following a power law. Small change in the relative cost of preventive to palliative treatment may result in big changes in this relationship. Addition of small world links narrows the range where the scaling (power) law is valid but the scaling persists for small values of detection and treatment times.

Methods

Model

We assume that individuals are located at nodes of a regular (square) lattice that represents geographical distribution of hosts. On this lattice, we define a local neighborhood of order z as a von Neumann neighborhood in which we include z shells and $\phi(z) = 2z(z + 1)$ individuals, excluding the central one. Accordingly, $z = 0$ corresponds to a single individual, which means that this individual is not in contact with anyone, $z = 1$ corresponds to 4

nearest neighbors while $z = \infty$ corresponds to the whole population in the limit of infinite size of the system. For the small world model a fixed number of long range links has been added to the regular network described above. Those links span the whole population, but otherwise behave like local links.

The epidemiological model is a standard SIR (Susceptible-Infected-Removed) model [13], modified to include pre-symptomatic and symptomatic stages of the disease and to account for detection and treatment (cf. fig. 1). All individuals are initially susceptible (**S**) and the epidemic is initiated by introduction of several infected (**I**), pre-symptomatic individuals. Each of infected individuals (symptomatic and pre-symptomatic) stays in contact with a given (fixed) number of other individuals in its infection neighborhood of order z_{inf} . After infection, the susceptible individual moves first to infected, pre-symptomatic class, (**I**) compartments. It can further infect its neighbors with probability f per a contact but cannot be treated yet. As symptoms develop with probability q , individual moves to **D** class and can be detected. It is still infectious but can spontaneously recover with probability r and accordingly, move to a recovery class, (**R**) and cannot be further infected or treated.

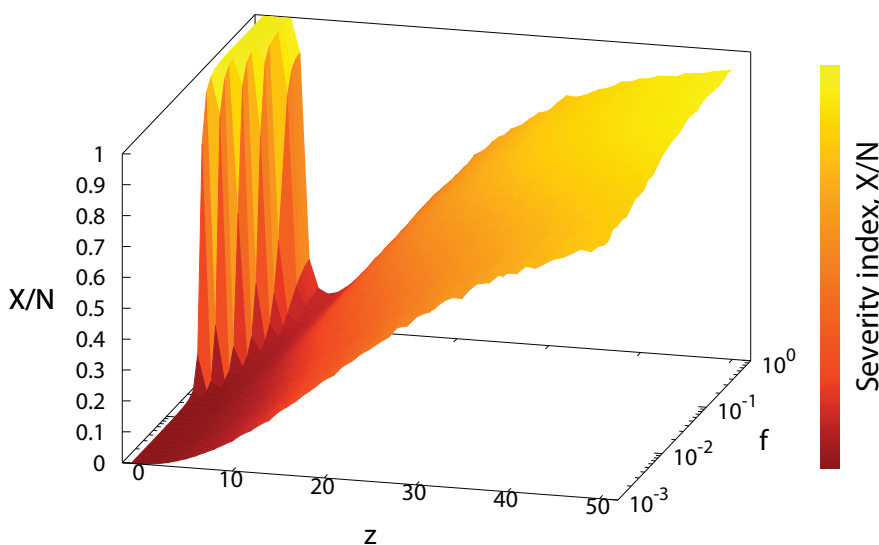


Figure 2. Severity index, X, as a function of the infection rate per contact f and the control neighborhood size z . Simulation parameters: $q = 0.5$, $v, r = 0.1$ with 40 initial foci and infected neighborhood size set to $z_{inf} = 1$, cost $c = 1$.
doi:10.1371/journal.pone.0036026.g002

Detection triggers the control process which becomes activated with probability v . In consequence, all individuals (except \mathbf{R}) within control neighborhood of size z centered at the detected host, transfer to the treated class \mathbf{V} . The order of control neighborhood z may be different from the order of infectious neighborhood z_{inf} and is typically larger. Accordingly, the group of individuals subject to the treatment is composed of at least one symptomatic and a mixture of susceptible and infected pre-symptomatic individuals. For convenience, we extend the definition of the neighborhood z to capture situations when no spatial control is applied ($z = -1$), or when the treatment is applied solely to the detected individual ($z = 0$).

Numbers of individuals in each class are denoted by S, I, D, R and V , respectively with $N = S + I + D + R + V$ being the total constant number of individuals in the population.

In order to investigate the optimal control strategy, we need to compare value of future benefits (reduction of infection cases) with the value of future and current costs associated with a particular choice of measures in disease control and treatment. In this paper we allocate the costs to two groups:

$$X(z, t = \infty) = R(z, t = \infty) + cV(z, t = \infty). \tag{1}$$

The first term represents the palliative cost and is associated with individuals who are not treated and therefore spontaneously move into the \mathbf{R} class. The second term describes costs associated with treatment of detected individuals and their neighbors and is assumed to be proportional to the number of treated individuals V . In the above formula c represents a cost of treatment relative to the cost of infection and z stands for the control neighborhood size.

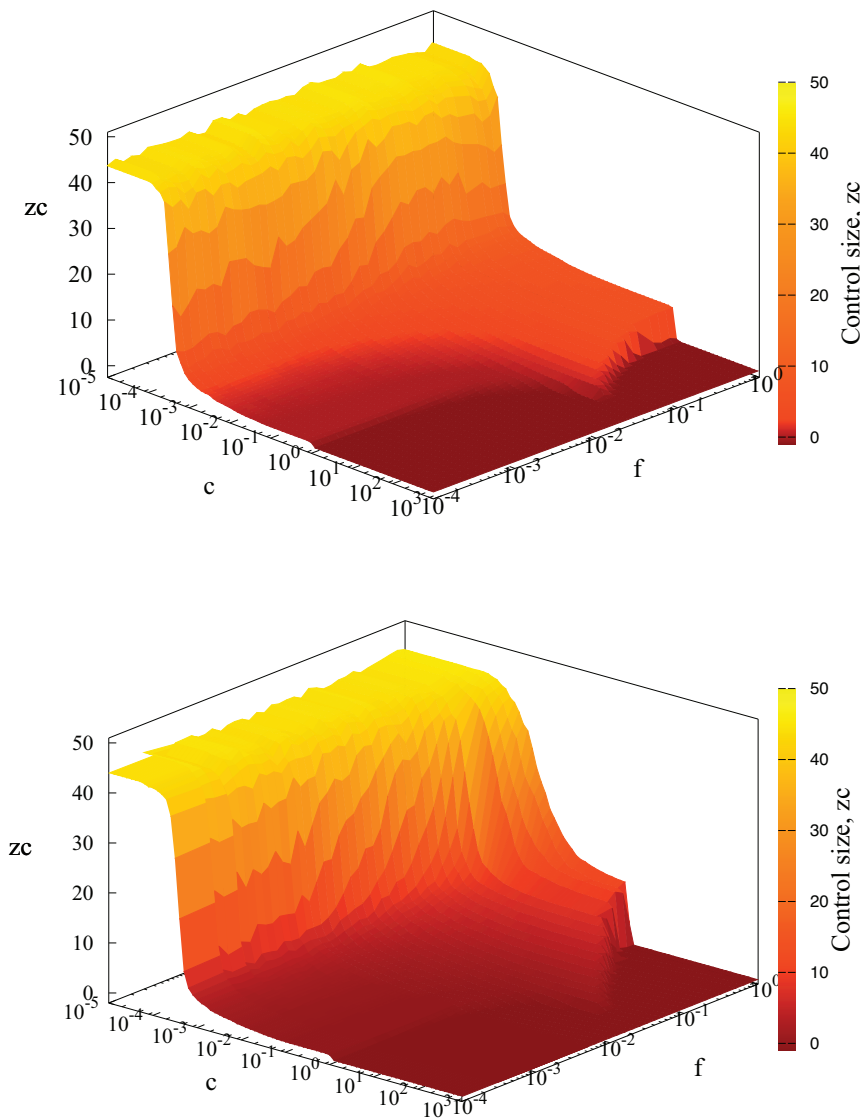


Figure 3. Control neighborhood size as a function of treatment cost c and infectiousness of the disease f for regular network and small world model. Simulation parameters: $q = 0.5, v, r = 0.1$, with 40 initial foci and $z_{inf} = 1$. Control size $z_c > 0$ represents local strategy (LS), $z_c = 0$ corresponds to the strategy when only the detected individual is treated and $z_c \geq 30$ denotes GS (more than 99% of individuals are treated). Null strategy corresponds to $z_c = -1$. Top figure denotes results for disease spreading on regular networks, whereas bottom to small world model with inclusion of additional 2000 number of long range links (5%). doi:10.1371/journal.pone.0036026.g003

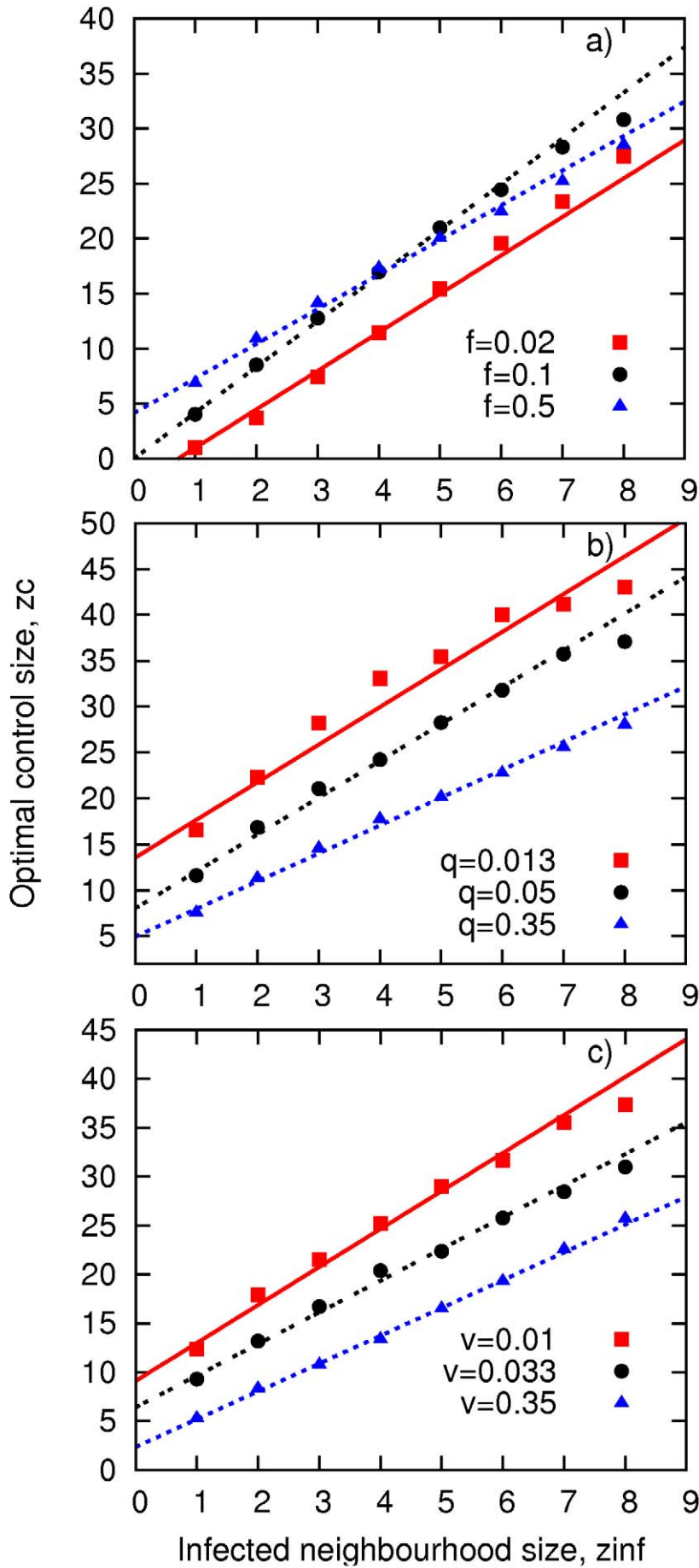


Figure 4. Relationship between z_c and z_{inf} for treatment cost $c=1$. Points mark the simulation results whereas lines correspond to fitted linear function $z_c = z_{inf} * a + b$. From top to bottom, the following sets of constant kinetic parameters have been assumed: (a) $q=0.5, v=0.1$, (b) $v=0.1, f=1$, (c) $q=0.5, f=1$. Errors (standard deviation from the mean) are too small to be visible. doi:10.1371/journal.pone.0036026.g004

Both estimates of R and V are evaluated at the end of each simulation run ($t \rightarrow \infty$).

Simulations

Monte Carlo simulations have been performed on a regular grid of 200 by 200 cells with periodic boundary conditions with and without long-range links. This choice of size has been dictated by a trade off between numerical efficiency and avoidance of small-size effects which could influence results. Additional numerical tests proved the consistency of results for different system sizes [12].

Epidemics have been initiated by addition of 40 infected individuals to an otherwise susceptible population. Each simulation run has been continued until $I(t) + D(t) = 0$ (i.e. up to the time when no further infection can occur). Subsequently the severity index X has been evaluated from the formula eq.(1). The optimal strategy is then determined by the minimal value of the severity index X_c . The corresponding value of z gives the optimal size of the control neighborhood, z_c (see fig. 2 for illustration). In the simulations, the minimization of the severity index is achieved by sweeping through different values of the control neighborhood size z , while keeping other parameters fixed. For each value of z only a single simulation has been performed. Collections of this results yield a dependence of X on z . A minimum value of X in this collection gives an estimate of X_c and the corresponding z gives an estimate of z_c . This procedure has been repeated 100 times to yield representative average values of z_c and X_c and their corresponding standard deviations.

Results

The long time ($t \rightarrow \infty$) behavior of the model in the absence of control (Null Strategy, NS, i.e. $z = -1$) is determined by the probability f of passing the infection to a susceptible node from any of its neighbors within the neighborhood size ranging from 4 ($z=1$) to 144 ($z=8$). For small f , the infection quickly dies out. Disease spreads invasively over the population for large f , when no control is applied, $X(z, \infty) \propto R(z, \infty) \simeq N$. When $z \geq 1$, the ratio R/N declines with the order of the control neighborhood. However, at the same time the number of treated individuals V increases, contributing to the total cost X , cf. eq.(1). For $c \neq 0$, $X(z)$ is either a monotonic function of z for small values of f or a non-monotonic function for highly contagious disease (large f , see fig. 2).

Three regions can be identified in the dependence of z_c on c and f , see fig. 3. For small values of c , Global Strategy (GS) is dominating, whereas for large c , it is best to refrain from treatment, Null Strategy (NS), fig. 3.

Although the location of the minimum of $X(z)$ varies with increasing f and c values (see figs. 2, 3), a relatively wide plateau region with an almost constant z_c develops for intermediate values of c and f and corresponds to the local strategy (LS), fig.3. The structure in fig. 3 is partially deformed by addition of long-range links, however, the plateaux persists for small values of f .

We have therefore focused on the plateaux region (LS) of z_c and have explored its dependence on epidemiological parameters: z_{inf}, q, v , with constant f and c . We have first explored dependence of z_c on the size of infection neighborhood for $c=1$, see fig. 4. The relationship can be accurately approximated by a linear function for a wide range of parameters, infectiousness f (fig.4a), the rate at

which symptoms appear, q (fig.4b) and the treatment rate, v (fig.4c) for $z_{inf} \in [1,8]$.

As already seen in fig. 3, infectiousness f hardly affects the slope and intercept of the linear relationship, fig.4a. Increasing q and v causes the lines to shift towards lower values of z_c , with major changes in the intercept but slope only slightly affected (cf. fig.4b,c). In contrast, the relationship between z_c and q (or v) for fixed z_{inf} is non-linear. It is more convenient to consider $1/q$ instead of q as $\tau_q = 1/q$ has an interpretation of average time till detection of symptoms. Similarly, $\tau_v = 1/v$ can be interpreted as an average time till treatment.

Broadly speaking, z_c increases with τ_q and τ_v , fig. 5. This is consistent with the following mechanism. Consider a single infected but pre-symptomatic individual. The disease focus centered on it will spread until appearance of symptoms after time τ_q . Thus, the longer it takes to discover symptoms of the disease, the farther the disease would spread from its original focus. As a consequence, the infected area becomes larger and so does z_c . Similarly, the longer time from detection until treatment, the further the disease moves away from original focus. As a result, the control size grows with increasing treatment time.

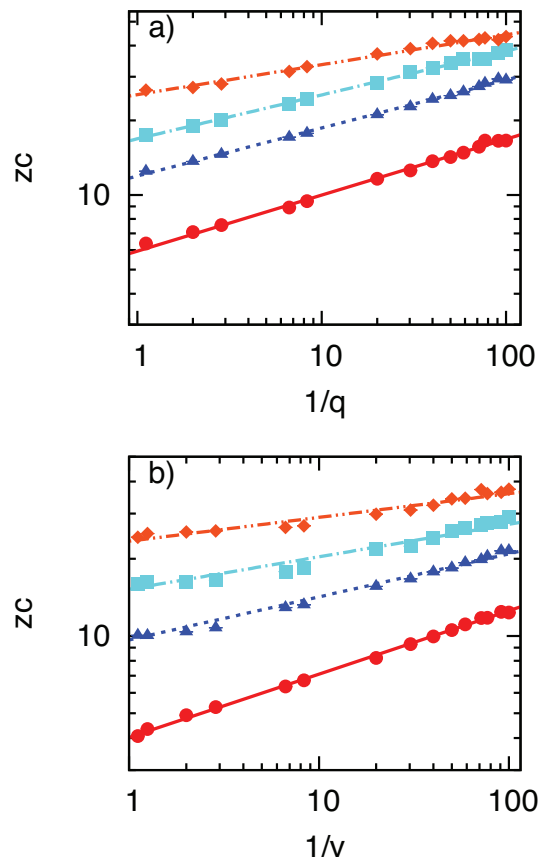


Figure 5. Relationship between z_c and τ_q in a) and τ_v in b). Points mark the simulation results and lines correspond to fitted functions: a): $z_c(\tau_q) = \alpha_q \tau_q^\beta$ and b): $z_c(\tau_v) = \alpha_v \tau_v^\beta$ for red: $z_{inf} = 1$, navy blue: $z_{inf} = 3$, blue: $z_{inf} = 5$, orange: $z_{inf} = 8$. doi:10.1371/journal.pone.0036026.g005

Intriguingly, it appears that z_c scales algebraically with τ_q (and with τ_v) following a power law: $z_c = \alpha_q \tau_q^\beta$ and $z_c = \alpha_v \tau_v^{\beta'}$ eq.(3) (see fig. 5) with exponents well below 1.

The exponents β , β' are similar for a range of z_{inf} within the plateau regime of an optimal control radius of the epidemic, (see fig.3), i.e. for $z_{inf} \in [1,8]$, $\beta \in [0.14,0.25]$ and $\beta' \in [0.10,0.27]$.

While fig. 5 is representative of results for $c \leq 1$, moving c just beyond $c=1$ causes a dramatic change in the $z_c(\tau_v)$ dependence for large values of τ_q and τ_v , corresponding to detection and vaccination time comparable with duration of epidemics (approximately 10^4 time steps for large values of τ_v and τ_q). The control neighborhood z_c decays abruptly for increasing times τ_q , τ_v , as illustrated in fig. 6. This change is associated with very inefficient control (long time till detection, $\tau_q \gg 1$ and long time from detection to treatment, $\tau_v \gg 1$). If the cost of control is lower or equal to the cost of palliative care, it is still better to treat, even

though we are not very efficient with treatment and most individuals are spontaneously removed. However, if the cost of vaccination is only marginally higher than the cost of untreated case, prevention is no longer cost-effective. We also note that it is only a combination of very long values of τ_q and τ_v that leads to a limited range of application of the scaling formulas ($z_c = \alpha_q \tau_q^\beta$ and $z_c = \alpha_v \tau_v^{\beta'}$).

The scaling region of z_c as a function of τ_q and τ_v also depends on c in a fashion reminiscent of fig. 3. For small values of c , Global Strategy of treating everybody is optimal regardless of the parameters, cf. fig. 3 with fig. 7. In contrast, Null Strategy is optimal for large c (figs. 3 and 7). The region where Local Strategy is optimal occupies the region near $c=1$, but it becomes narrower when the disease is more infectious (fig. 3) or when the control is less efficient (for increasing values of τ_q (fig. 7a) and τ_v (fig. 7b)). Within this region, z_c is given by scaling formulas. As seen before,

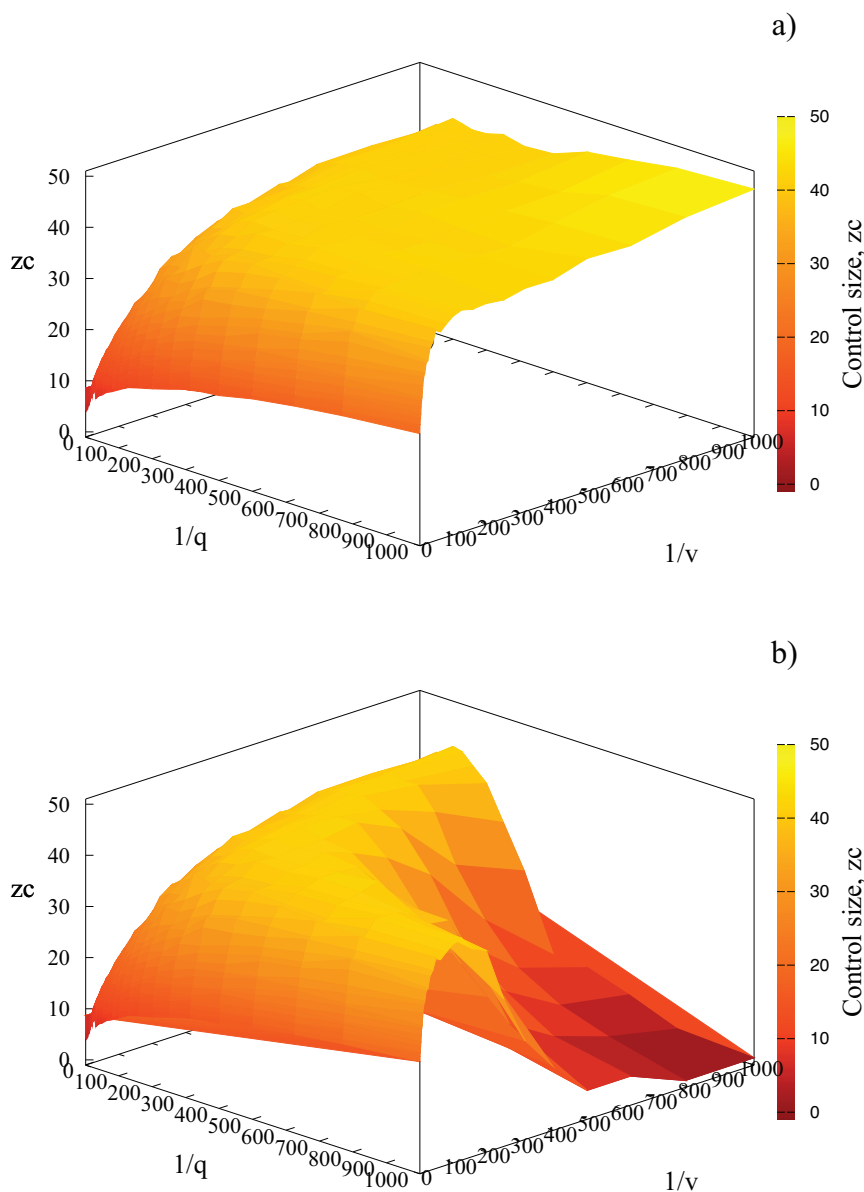


Figure 6. Control neighborhood size as a function of both detection time, τ_q , and recovery time, τ_v , for $c=1$ in a) and $c=1.001$ in b). Simulation parameters: $f=0.1$, $r=0.1$, $z_{inf}=1$, 40 initial foci. doi:10.1371/journal.pone.0036026.g006

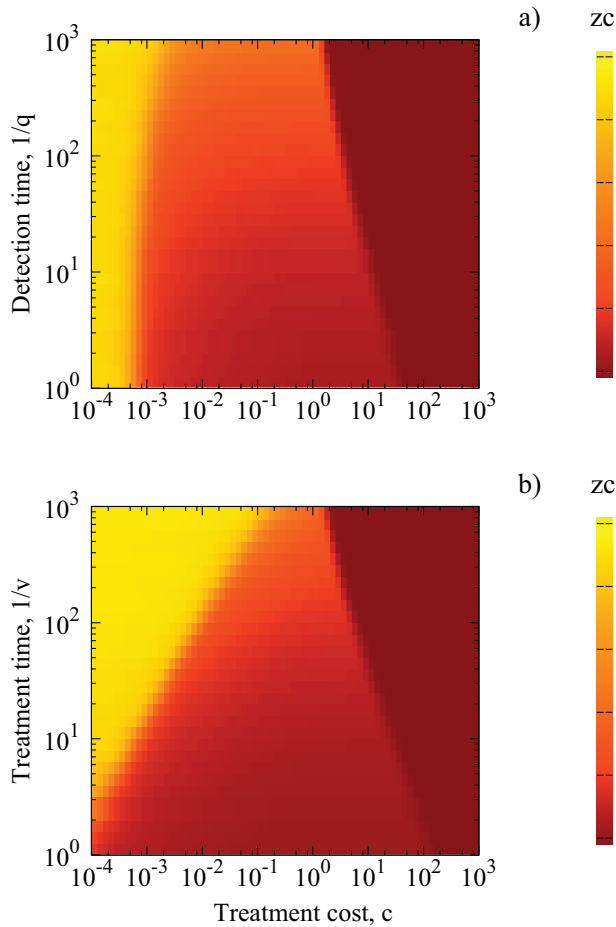


Figure 7. Control neighborhood size as a function of treatment cost c and detection time τ_q (a) and treatment time τ_v (b). Simulation parameters: $f=1$, $q=0.5$, $v,r=0.1$, with 40 initial foci and $z_{inf}=1$. Color borderlines between different regions indicate transition regions among various optimal strategies. doi:10.1371/journal.pone.0036026.g007

$c=1$ is a special case asymptotically associated with a breakdown of LS for very large or very small f (fig. 3) and very large values of τ_q and τ_v (fig. 7).

The addition of long range links shifts the optimal radius of control towards larger values, figs. 3, 8. The scaling behaviour (cf. fig.5) is characteristic for a regular network and changes when long-range bonds is added (see fig.8). With 400 random long-range contacts (corresponding to 1% of all links) the scaling relation between z_c and τ_q (τ_v) breaks down for detection (treatment) times exceeding 10. This is clearly indicated by deviation of the results from red bottom line (in fig.8) denoting simulation data for regular networks (the same as in fig. 5). Altogether, addition of small world links reduces the range of detection τ_q and treatment τ_v times for which the power law relationship is valid. This is caused by long range links allowing disease to escape from the local control. In contrast, if we are able to detect disease quicker, it has not much chance to escape and the disease spread is effectively short range. Consequently, the scaling can be observed for small values of detection and treatment times, τ_q, τ_v . In summary, with increasing degree of randomness of networks (larger number of links) not only the control radius rises but also the scaling disappears. Note that the dashed black line, $z_c=40$ in fig. 8, represents Global Strategy.

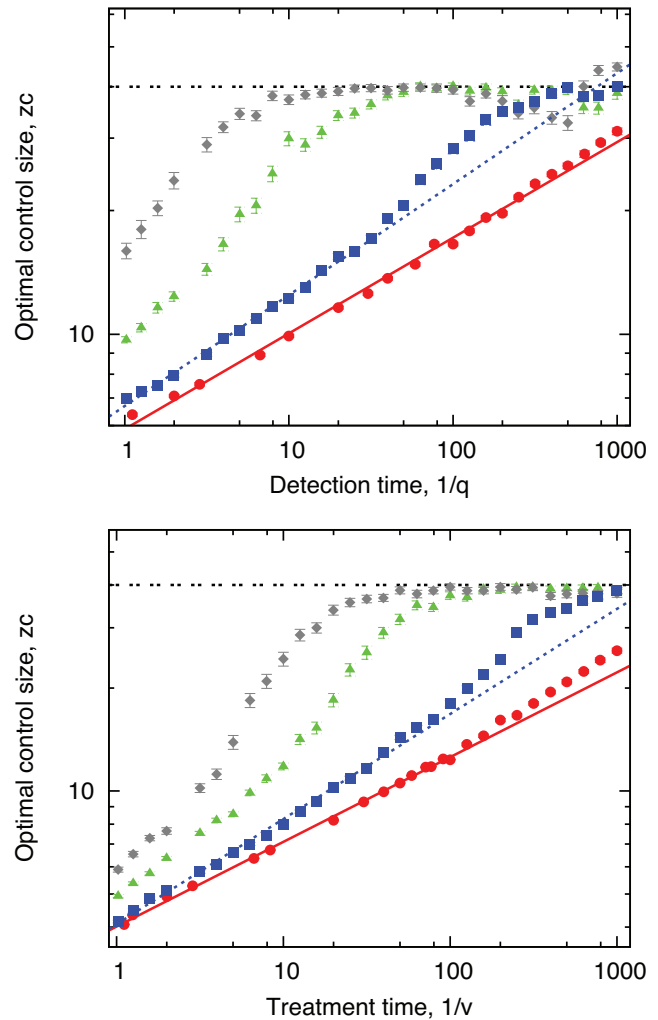


Figure 8. Relationship between z_c and τ_q on top and τ_v on bottom for regular and small world network with varying number of long-range links. Lines and simulation points from bottom: red: regular network, navy blue: small world with additional 1% of links, green: small world with additional 5% of links, grey: small world with additional 10% of links, dashed black: $z_c=40$ which corresponds to treating the whole population. Simulation parameters: $f=1$, $v,r=0.1$, $z_{inf}=1$, 40 initial foci, 1%,5%,10% of long-range links. doi:10.1371/journal.pone.0036026.g008

Discussion

In order to design a successful strategy for controlling a disease we need to take into account not only epidemiological and social factors (including the topology of the social network of contacts and in particular z_{inf}), but also economic considerations. Some of these factors might be unknown or hard to estimate, particularly in real time as the epidemic unfolds. It is therefore crucial to understand the relationship between the optimal control strategy and parameters, for a wide range of possible values. It is even more important to establish those processes and parameters to which a selection of optimal strategy is not particularly sensitive, as this allows us to find strategies that can be designed in advance, even without knowing their actual values for a given emerging disease.

Regular networks have been traditionally used for modelling epidemic outbreaks of human, animal and plant diseases [14,15] and many variants of such an approach (with e.g. constant or

randomized probabilities of infection passed to neighbouring nodes on a grid) have been studied. However, an accumulated experimental evidence demonstrates that real systems rarely follow this kind of idealization being neither completely random nor located on regular lattices. Among other types of networks that have been the object of intense studies are the small-world and scale-free networks. In particular, the small world network with randomly chosen shortcuts between the nodes, is considered a model well extrapolating between extremes like regular and random network. It has been also preferentially used by modellers describing outbreaks of disease starting simultaneously in different regions of the world (propagation of the SARS virus, [16]). Accordingly, in order to assess the occasional long distance dispersal of the disease, we have also considered small world links, representing e.g. random transport by wind or by plane.

In our previous paper we have shown that for a given set of z_{inf} , q and v , the broad choice of the strategy is determined by the relative cost of the treatment, c . For small values of c , GS is optimal, for large values of c , NS. Close to $c = 1$, a LS dominates and the detailed value of the control neighborhood z_c depends on the epidemiological parameters, although not on f in a wide range. In this paper we extend this analysis to include other epidemiological parameters. In particular we show that the broad division between GS (for $c \ll 1$), NS (for $c \gg 1$) and LS (for $c \simeq 1$) holds for a wide range of parameters q and v (inverse of time to detection and inverse of time to treatment, respectively), fig. 7.

Three other key results emerge from our analysis. Firstly, it is very important to match scale of control to the scale of infection dispersal. This has already been seen in other papers [17], but this is the first time we show it for spatial control on networks in the presence of economic evaluation. However, we also show that the size of the control neighborhood is not just simply equal to the size of the infection neighborhood (see fig. 4 and compare the scale of horizontal and vertical axes). In the presence of pre-symptomatic individuals ($\tau_q \gg 0$) and in the face of delays associated with application of control ($\tau_v \gg 0$) we need to extend z_c well beyond z_{inf} . The relationship between z_{inf} and z_c is one of the key formulas for planning response to epidemics. It enables authorities to plan actions aiming at eradication of the disease by setting a sufficiently large – but not too large – zone of eradication around each detected case. Traditionally, such recommendations are based on the dispersal patterns of the disease, although increasingly simulation models are used. This procedure has led to establishment of the 1,900ft rule for citrus canker [18] whereby all citrus trees are cut down within this radius from every affected tree and the 3 km/10 km rule for foot-and-mouth disease [19].

References

- Newman M (2010) Networks: an introduction. Oxford Univ Pr.
- Keeling M (2005) Models of foot-and-mouth disease. Proceedings of the Royal Society B: Biological Sciences 272: 1195.
- Gastner M, Newman M (2006) Optimal design of spatial distribution networks. Physical Review E 74: 016117.
- Barrett S (2003) Global disease eradication. Journal of the European Economic Association 1: 591–600.
- Rowthorn R, Laxminarayan R, Gilligan C (2009) Optimal control of epidemics in metapopulations. Journal of the Royal Society Interface 6: 1135.
- Ndeffo Mbah M, Gilligan C (2010) Optimization of control strategies for epidemics in heterogeneous populations with symmetric and asymmetric transmission. Journal of Theoretical Biology 262: 757–763.
- Ferguson N, Donnelly C, Anderson R (2001) The foot-and-mouth epidemic in Great Britain: pattern of spread and impact of interventions. Science 292: 1155.
- Klein E, Laxminarayan R, Smith D, Gilligan C (2007) Economic incentives and mathematical models of disease. Environment and Development Economics 12: 707–732.
- Gersovitz M, Hammer J (2004) The Economical Control of Infectious Diseases*. The Economic Journal 114: 1–27.
- Boccara N, Cheong K, Oram M (1994) A probabilistic automata network epidemic model with births and deaths exhibiting cyclic behaviour. Journal of Physics A: Mathematical and General 27: 1585.
- Kleczkowski A, Dybiec B, Gilligan C (2006) Economic and social factors in designing disease control strategies for epidemics on networks. Arxiv preprint physics/0608141.
- Kleczkowski A, Oleś K, Gudowska-Nowak E, Gilligan C (2011) Searching for the most cost-effective strategy for controlling epidemics spreading on regular and small-world networks. Journal of The Royal Society Interface.
- Anderson R, May R (1991) Infectious diseases of humans: dynamics and control. Wiley Online Library.
- Jeger M, Pautasso M, Holdenrieder O, MW S (2007) Modelling disease spread and control in networks: implications for plant sciences. New Phytologist 174: 279–297.
- Shirley M, Rushton S (2005) The impacts of network topology on disease spread. Ecological Complexity 2: 287–299.
- Small M, Tse C, Walker D (2006) Super spreaders and the rate of transmission of the SARS virus. Physica D 215: 146–158.

However, our results show that the relationship between z_c and z_{inf} is non-trivial and in particular it involves non-linear functions of τ_q and τ_v . Although we are still far from being able to provide a formula relating z_c to all epidemiological parameters, our result stresses importance of using models to design control strategies [20].

We also show that $c = 1$ is a special case. In particular, we show high sensitivity of z_c to changes in c for large values of τ_q and τ_v . Thus, if the symptom detection time (τ_q) and reaction time (τ_v) are both long, small change in c leads to very big changes in z_c , see fig. 6 and 7. Without knowing the exact value of c it is therefore very difficult to design the strategy in this case. Suppose we believe that $c > 1$ and therefore we chose a small value of z_c based upon fig. 6b. However, if in reality $c \leq 1$ (although very close to 1), z_c should be close to 50 (fig. 6a). This shows the importance of knowing what the actual value of c is [12] estimated that for vaccination $c = 0.01–0.85$, but can be larger than 1 for culling.

In this paper we have used regular and small world networks to describe the topology of interaction between individuals. Addition of small world links into population narrows the range where the scaling (power law) relationship of z_c on τ_q and τ_v is valid but the scaling persists for small values of detection and treatment times.

Our studies can also be extended in other ways. The current work assumes relatively short overall time length of each epidemic and so no discounting is applied when the costs and benefits are estimated. We also assumed that the strategy is unchanged throughout the epidemic and that the network structure is static and relatively simple. Each of these assumptions can be relaxed. Discounting is often used in economics, but we expect for it to have a small impact on our results. Adapting the strategy to the current status of the epidemic often leads to a bang-bang solution [21], similar to our distinction between NS and GS.

Finally, a lot of attention have been recently given to non-local and random networks (small-world or scale-free networks) [12,22], to dynamic networks [23], and networks with random parameters [24]. Further extension of this work to include static and dynamic disorder is in progress.

Acknowledgments

We are very grateful to Bartek Dybiec for useful discussions.

Author Contributions

Conceived and designed the experiments: AK KO. Performed the experiments: KO. Analyzed the data: KO EGN AK. Contributed reagents/materials/analysis tools: KO EGN AK. Wrote the paper: KO EGN AK.

17. Gilligan CA, Truscott JE, Stacey AJ (2007) Impact of scale on the effectiveness of disease control strategies for epidemics with cryptic infection in a dynamical landscape: an example for a crop disease. *Journal of the Royal Society Interface* 4: 925–934.
18. Gottwald TR, Hughes G, Graham JH, Sun X, Riley T (2001) The citrus canker epidemic in Florida: the scientific basis of regulatory eradication policy for an invasive species. *Phytopathology* 91: 30–4.
19. DEFRA website. Available: <http://animalhealth.defra.gov.uk/managing-disease/notifiable-disease/footand-mouth.html>. Accessed 2012 Apr, 3.
20. Kao RR (2002) The role of mathematical modelling in the control of the 2001 FMD epidemic in the UK. *Trends In Microbiology* 10: 279–286.
21. Forster GA, Gilligan CA (2007) Optimizing the control of disease infestations at the landscape scale. *Proceedings of the National Academy of Sciences of the United States of America* 104: 4984–4989.
22. Dybiec B, Kleczkowski A, Gilligan CA (2004) Controlling disease spread on networks with incomplete knowledge. *Physical Review E* 70.
23. Vernon MC, Keeling MJ (2009) Representing the UK's cattle herd as static and dynamic networks. *Proceedings of the Royal Society B-Biological Sciences* 276: 469–76.
24. Taraskin SN, Ludlam JJ, Neugebauer CJ, Gilligan CA (2005) Extinction of epidemics in lattice models with quenched disorder. *Physical Review E* 72.